



# Enhancement of quality of modal test results of an unmanned aerial vehicle wing by implementing a multi-objective genetic algorithm optimization



Nima Pedramasl<sup>a</sup>, Melin Şahin<sup>a,\*</sup>, Erdem Acar<sup>b</sup>

<sup>a</sup> Department of Aerospace Engineering, Middle East Technical University, 06531, Ankara, Turkey

<sup>b</sup> Department of Mechanical Engineering, TOBB University of Economics and Technology, 06560, Ankara, Turkey

## ARTICLE INFO

### Article history:

Received 8 December 2016  
Received in revised form 3 May 2017  
Accepted 26 September 2017  
Available online 2 October 2017

### Keywords:

Modal test  
Pre-test planning  
UAV wing  
Genetic algorithm  
Multi-objective optimization  
Pareto frontier curves  
Experimental validation

## ABSTRACT

Due the fact that aircraft structures work in an environment with lots of dynamic forces, it is of vital importance to perform a dynamic analysis to understand dynamic characteristics of aircraft in that specific environment. These characteristics are usually obtained using numerical methods (finite element analysis) or experimental methods (classical modal analysis). In classical modal analysis, quality of test equipment plays a critical role in final results' accuracy and completeness. There is another important factor which is expertise of a test engineer. Test engineer uses his/her experience to find sufficient/optimum numbers, types and locations of transducers. This process sometimes would be time consuming and exhausting which results in degradation of test results quality. In this paper an algorithm is developed and implemented to find numbers, types and locations of transducers in a modal test which will make results of test more reliable. In this study, an unmanned aerial vehicle used as dummy structure to test functionality of developed algorithm. This algorithm utilized two toolboxes from MATLAB (multi-objective genetic algorithm toolbox and parallel computing toolbox) and MSC© NASTRAN finite element solver. A genetic algorithm based optimization is performed in which MSC© NASTRAN was used to calculate dynamic characteristics of UAV wing. Since this was a time and resource consuming process a parallel computing cluster is also utilized which decreased run times at least fourfold. In algorithm it was tried to find optimum numbers, types and locations of transducers which will result in minimum cost and error in test results. Error was defined as a summation of mode shape observability error, mass loading error and optimum driving point error. At the end of study optimization results are presented and validated by classical modal analysis.

© 2017 Elsevier Masson SAS. All rights reserved.

## 1. Introduction

In literature, studies related to finding optimum location of transducers in modal test can be traced back to the end of 1970s. Shah and Udwardia [1] assumed that the error in prediction of dynamic parameters of a system follows Gaussian distribution. They also assumed that correlation between errors of transducers was proportional to distance between them, and the mean value of error was taken as zero. They constructed a correlation matrix which embed correlated error between transducers. Using a random search optimization algorithm, a norm (trace, determinant, etc.) of this matrix was minimized for a given number and types of transducers. The other works done in 1990s, instead of corre-

lated error matrix, Fisher information matrix (FIM) was used in optimization and a norm of this matrix (trace, determinant, etc.) was maximized, because maximum norm value of Fisher information matrix corresponds to minimum norm value of correlated error matrix for optimum location of transducers. While Kammer [2], Yao [3] and Udwardia [4] did not include the correlated error between transducers, Kirkegaard and Brinckera [5] included transducers' correlated error in their optimization. Kammer [2], Udwardia [4] and Kirkegaard and Brinckcker [5] used local search optimization algorithm, whereas Yao [3] used genetic algorithm. Based on Fisher information matrix, there were two commonly used methods which were effective independence (EI) and modal kinetic energy (MKE). In effective independence method the effect of transducers location on orthogonality of interested mode shapes was studied and in modal kinetic energy, the amount of added kinetic energy to modes of interest by transducers' location was studied. Penny [6] compared the Fisher information matrix

\* Corresponding author.

E-mail addresses: pedramasl@gmail.com (N. Pedramasl), msahin@metu.edu.tr (M. Şahin), acar@etu.edu.tr (E. Acar).

and Guyan reduction methods and found that Fisher information matrix was more effective. In all of above studies, it was tried to find optimal location of a specific set of transducers and there were no functional relation between modal characteristics of structure with the type or number of transducers. Even though most of these studies used genetic algorithm for optimization, particle swarm optimization (PSO) method was also used. There also exist other studies where a hybrid optimization algorithm was used. For example, Rao and Anandakumar [7] used PSO as global optimization routine and Nelder–Mead method as local optimization routine.

In all of above studies dynamic characteristics of structure were found using fully analytical or semi-analytical methods. There also exist other studies that used finite element solver. Langehove and Brughmans [8] used MSC® NASTRAN and LMS/PRETEST software packages to find optimal location of transducers over NASA's X33 suborbital spaceplane. Similarly, Peck and Torrens [9] used DMAP (Direct Matrix Abstraction Program) which is scripting language of MSC® NASTRAN. They used effective independence and average kinetic energy methods to reduce number of initial candidate transducers' location to optimum ones. In literature, usually it was tried find optimum location for a set of candidate transducer location. Types of transducers has also importance on quality of measured data. For example using a tri-axial accelerometer may correspond to using three uniaxial accelerometers to capture desired mode shape. In this way mass loading error of transducers could be reduced due to the use of one instead of three transducers. Selection of transducer type also helps in using high quality accelerometers which have lower biased error in their readings.

To the best of the author's knowledge, the sensor positioning studies in literature have been focused on optimal positioning of a given number of sensors of given type, whereas simultaneous optimization of the number of sensors, sensor types and sensor positions have not been investigated. The main objective of this study is to fill this gap in literature. To simplify the analysis, the error in prediction of the dynamic characteristics of the structure is limited to the mass loading error (error in the predictions of the first four natural frequencies of the structure caused by the sensor mass) and mode shape observability error in this study. The paper is structured as follows. The importance of pre-test analysis in modal testing is discussed first and a brief introduction to theoretical concepts is given. Next, finite element analysis (FEA) of the fin-like structure is presented. In finite element model, transducers are modelled as lumped mass over nodes. Since FEA solutions does not usually represent dynamic characteristics of modelled structure exactly, a modal test is performed to validate FEA results. Using FEA and test results, a correlation analysis is performed to evaluate reliability of numerical model. Due to some discrepancies between numerical and test models, a model updating is performed to increase the accuracy of the numerical model. Then, design variables, objective and constraint functions used in optimization problem are defined. Since optimization requires repetitive generation of the finite element model, a script is developed in MATLAB [10] which is capable of handling communications between the optimizer (MATLAB genetic algorithm toolbox module) and finite element solver (MSC®NASTRAN [11]). To speed-up the optimization process, a parallel processing algorithm is also implemented using distributed computing toolbox in MATLAB. To validate results obtained thorough optimization, modal tests are performed for various selected optimum configurations over Pareto frontier set. Finally, the paper culminates with concluding remarks followed by potential future research directions. Authors of this paper also applied same procedures and methodologies to a different test structure (fin plate) and it was presented at 16th AIAA/ISSMO Multidisciplinary Analysis and Optimization Conference [12].

## 2. Pre-test analysis theory

Quality of data obtained during a modal test is highly dependent on location of excitation, suspension and measurement points over test structure. Therefore it is very important to perform a pre-test analysis before modal test. Using equation of motion of a system with hysteresis damping model, receptance frequency response function  $\alpha(\omega)$  is derived and shown in Equation (1).

$$\alpha(\omega) = \frac{X(\omega)}{F(\omega)} = \frac{1}{-m\omega^2 + i\omega h + k} \quad (1)$$

In Equation (1),  $X$  and  $F$  are displacement and force values respectively.  $m$  is mass,  $k$  is stiffness and  $h$  is structural damping and  $\omega$  is frequency of excitation force. Receptance of system can also be written in terms of mass normalized eigenvectors  $\phi_{jr}$  and natural frequencies  $\omega_r$  of system which is shown in Equation (2).

$$\alpha_{jk}(\omega) = \sum_{r=1}^m \frac{\phi_{jr}\phi_{kr}}{\omega_r^2 - \omega^2 + ih\omega_r} \quad (2)$$

When a system is excited near one of its mode's natural frequency, that mode shape will have major contribution to total response of system which is shown in Equation (3).

$$X(\omega_r) = \alpha(\omega_r)F(\omega_r) \cong \frac{\phi_{jr}\phi_{kr}}{ih\omega_r^2} F(\omega_r) \quad (3)$$

As it is evident from Equation (3), amplitude of response of system is proportional to modal constant and natural frequency of that specific mode.

$$X(\omega_r) \propto \frac{\phi_{jr}\phi_{kr}}{\omega_r^2} \quad (4)$$

Same equation can also be derived for displacement, velocity and acceleration.

$$\begin{aligned} X(t) &= X(\omega)e^{i\omega t} X(\omega_r) \propto \frac{\phi_{jr}\phi_{kr}}{\omega_r^2} \\ \dot{X}(t) &= i\omega X(t)\dot{X}(\omega_r) \propto \frac{\phi_{jr}\phi_{kr}}{\omega_r} \\ \ddot{X}(t) &= -\omega^2 X(t)\ddot{X}(\omega_r) \propto \phi_{jr}\phi_{kr} \end{aligned} \quad (5)$$

In the case where excitation and response are at same point,  $\phi_{jr}\phi_{kr}$  term in Equation (5) will be  $\vartheta_{jr}^2$ . Using these response amplitudes of displacement, velocity and acceleration three indicators (ADDOFD, ADDOFV, ADDOFA) [13] are going to be used in this study which are shown in Equation (6).

$$\text{ADDOFD}(j) = \sum_{r=1}^m \frac{\vartheta_{jr}^2}{\omega_r^2} \quad m = 1, 2, 3, \dots, n \text{ (modes of interest)}$$

$$\text{ADDOFV}(j) = \sum_{r=1}^m \frac{\vartheta_{jr}^2}{\omega_r} \quad m = 1, 2, 3, \dots, n \text{ (modes of interest)}$$

$$\text{ADDOFA}(j) = \sum_{r=1}^m \vartheta_{jr}^2 \quad m = 1, 2, 3, \dots, n \text{ (modes of interest)}$$

$\vartheta_{jr}$  = modal constant at  $j$ th DOF of  $r$ th mode

ADDOFD = Average Driving Degree of Freedom Displacement

ADDOFV = Average Driving Degree of Freedom Velocity

ADDOFA = Average Driving Degree of Freedom Acceleration (6)

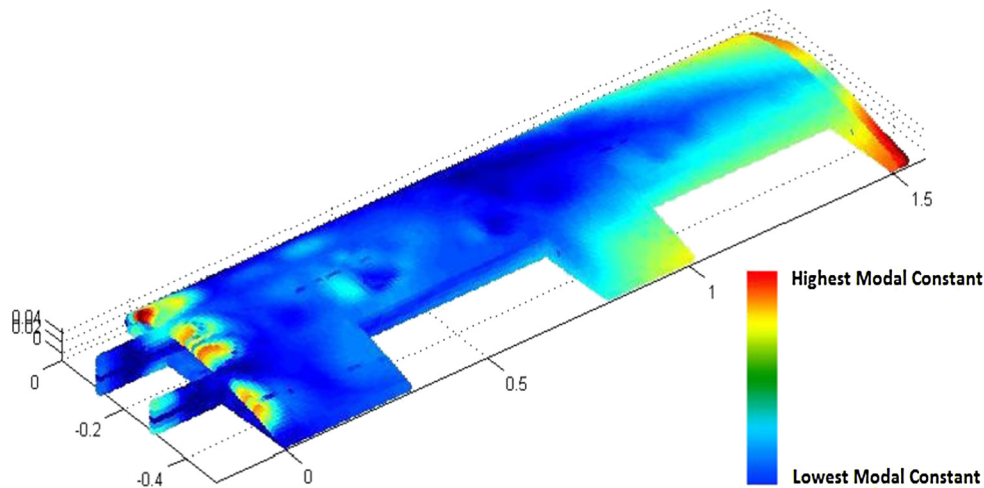


Fig. 1. Contour plots for minimum modal constant (first four modes). (For interpretation of the colours in this figure, the reader is referred to the web version of this article.)

### 2.1. Excitation location

During energy transfer from one or multiple point using exciter several measures must be taken to get high quality test results.

- Frequency content of force
- Amplitude of force
- Avoiding adverse effect of excitation equipment's on test results

While exciting a structure, to observe modes of interest in test results it is obligatory to send out a force with frequencies of those modes. In impact hammer case, frequency spectrum of force can be controlled by changing tip of impact hammer (rubber, plastic and aluminium) and in modal shaker case, frequency band of interest are swept using sine sweep method or a white noise signal is used to excite a band of frequencies at same time.

Transfer of sufficient energy to structure will be ensured by the amplitude of the applied force. When the energy transfer is considered, it is suggested that in all modes of interest the structure be excited from locations where highest modal constant are observed (because more impact energy will be transferred into kinetic/strain energy rather than into heat and sound). Of course double-hit or shaker-structure interaction will be present as a downside of this approach. So as a rule of thumb it will be practical to excite structure from locations close to nodal lines considering they are regions with lowest velocity and acceleration. However, it must be noted that this requires forces with higher amplitude so that sufficient energy can be delivered into the structure.

The last but not the least is “the excitation equipment's adverse effect on test results”. The issues that will be encountered are related to impact hammer and modal shaker. Considering the impact hammer, double hit issue is observed which occurs while exciting structure from locations with high velocity amplitude. Whereas for modal shaker the structure-shaker interaction issue will be encountered (because force transducer attached to structure which introduce extra mass to system) and it is observed while exciting structure from locations where high acceleration amplitude exist. Thus; it is practical to excite structure from regions near to nodal lines which can be achieved by obtaining the location with minimum ADDOFV and ADDOFA. Hopefully these areas correspond to locations with minimum modal constant. Contour plot

of modal constants (average of the first four modes) is represented in Fig. 1.

### 2.2. Suspension location

Structure motion will not be restrained, when a structure is suspended from locations near nodal lines of a particular mode in a free-free test. Thus the minimum value of the ADDOFD for all interested modes can be used to select optimum suspension locations. The wing in this study is considered a fixed-free problem as it is clamped by a set of four nuts and bolts connection from spar to base, and as a result there is no need for suspending the structure.

### 2.3. Measurement location

Placing accelerometers on the optimum locations over structure during modal test, makes it possible for test engineer to observe all of interested mode shapes in results. These optimum locations are usually location with highest acceleration. Placing accelerometers over these areas also increases signal to noise ratio which in return increases quality of test results. Locations on structure with highest value of ADDOFA are marked as possible optimum location for accelerometers.

### 2.4. Finite element model reduction

Having motioned about the pre-test analysis prior to the actual modal tests, there is a need for the test model as correlation between mode shapes of the experimental model and that of the full finite element model is required for the optimization procedure. Since in each iteration of the optimization, it is practically impossible to perform modal tests to obtain an experimental model, a reduced finite element model is used as a resemblance of an experimental model. Therefore, in order to validate a finite element model a correlation study was performed. Correlation study is to find differences between the finite element model and the test model. Correlation is only possible when number of degrees of freedom of test and FE model are the same and in most of cases, finite element model will have more degrees of freedom than the test model. This can be remedied by applying a model expansion of test model or model reduction of finite element model. FE model was reduced using Guan reduction and in the reduction process some degrees of freedom are retained (master DOF) and the rest are discarded (slave DOF). The reduced system is solved for modal



Fig. 2. Unmanned aerial vehicle designed and manufactured in TÜBİTAK 107M103 project.

characteristics and it's found that natural frequencies are a little higher respect to original system and that's because of dropping inertial terms. In Guyan reduction method, the accuracy of results from reduced finite element model relies on the location of master DOF (measurement locations) [14,15].

While selecting master DOF three main criteria must be considered.

- Accuracy
- Completeness
- Practicality

Accuracy shows exactness of modal characteristics results obtained from reduced finite element model. Completeness checks whether all modes of interest are present in results of reduced model. For example if master DOF are chosen to be on nodal lines of a specific mode shapes, that mode shape won't be recognized in final results. But some DOF are excitation location therefore is obligatory to choose them as master DOF and not neglect them. Practicality ensures that areas which are out of reach or hard to reach are avoided to be selected as master DOF. In this study, cross modal assurance criteria matrix (Equation (7)) is used as an indicator to check accuracy and completeness of reduced finite element model. If master degrees of freedom are placed over optimal locations, diagonal elements of xMAC matrix will get closer to unity and off-diagonal get closer to zero which is a sign of high level of correlation between mode shapes (eigenvectors) of both full and reduced models.

$$\text{Cross MAC Matrix} = \frac{[[\emptyset_R]^T [\emptyset_F]]^2}{[[\emptyset_R]^T [\emptyset_R]][[\emptyset_F]^T [\emptyset_F]]}$$

$$[\emptyset_F] = \text{Mass Normalized Modal Matrix of Full FEM}$$

$$[\emptyset_R] = \text{Mass Normalized Modal Matrix of Reduced FEM} \quad (7)$$

Briefly, this whole aforementioned correlation process is actually performed to check whether the selected transducer's configuration is able to capture all interested mode shapes or not. Hence, the error in the reduction algorithm is further used as an indicator for the selection of the measurement points on the actual test structure.

### 3. UAV wing

Unmanned aerial vehicles (UAV) are a kind of drones which are mainly controlled in two ways which are remotely controlled (RC) and computer controlled (Autonomous). Endurance and range of these drones are the most important performance goals in design stage. Therefore they are very light weight and flexible which makes them more prone to vibration borne problems. In order to

Table 1  
Mesh convergence analysis.

Mode shape	1st mesh	2nd mesh	3rd mesh
(Element Edge Length)	(0.01 m)	(0.005 m)	(0.0025 m)
1st Out-of-Plane Bending [Hz]	15.43	15.13	14.99
1st In-Plane Bending [Hz]	50.51	50.12	49.87
1st Torsion [Hz]	64.41	63.15	62.68
2nd Out-of-Plane Bending [Hz]	97.05	95.35	94.86
# of Elements	35580	70491	140313
# of Nodes	18764	37575	73993
% Difference with 1st Mesh Density	–	1.98	0.93

solve these problems ground vibration tests (GVT) are usually performed on UAVs to find dynamic characteristics of aircraft before going airborne. Using these GVTs, a structural design engineer is able to modify structure in a way which leads to lower vibrational problems. This is strongly dependant on quality and reliability of GVTs. To have that it is required to perform a pre-test analysis before those modal tests. In this study wing of an UAV which is shown in Fig. 2 was used as test specimen. This UAV was designed and manufactured in a project which was funded by TÜBİTAK institute (TÜBİTAK 107M103).

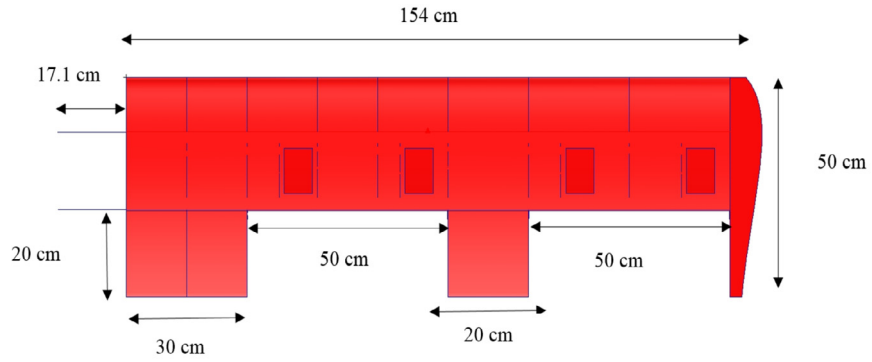
#### 3.1. Finite element modelling and analysis of the UAV wing

UAV wing is modelled and meshed using MSC® PATRAN [16] (Fig. 3). Modal characteristics of the wing (i.e. the natural frequencies and the corresponding mode shapes) are determined by MSC® NASTRAN using SOL103 module and are shown in Fig. 4. A mesh convergence analysis is also performed to obtain a fine enough mesh density with reasonable accuracy and computing time. Different mesh densities are depicted and the mesh convergence analysis results are tabulated in Table 1. It can interpreted from the table that increase in mesh density over 0.0025 (3rd Mesh Density) results in differences smaller than 0.93% in predictions, therefore 3rd mesh density (0.0025 m) is decided to be used in this study.

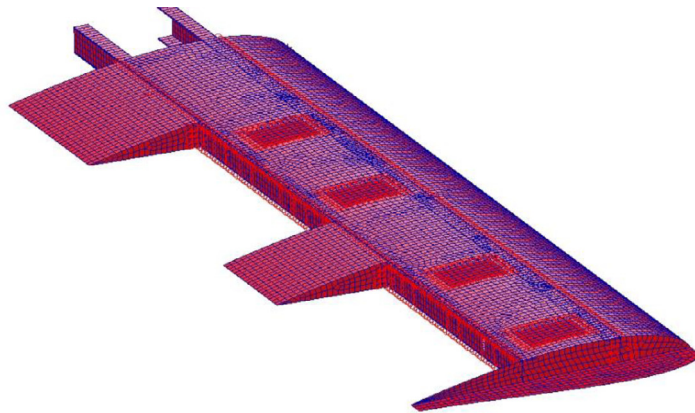
#### 3.2. Test model of the UAV wing

To find modal characteristics of the UAV wing a classical modal analysis (CMA) is performed. A miniature accelerometer (B&K 4517-002) [18] is mounted on tip of the wing and it is excited using an impact hammer (B&K 8206) [17] with aluminium tip. Accelerance frequency response functions (FRFs) are extracted by performing roving hammer test. B&K 7753 (Modal Test Consultant w/ six channels) [20] data acquisition device is used to collect data from sensors and B&K Pulse® LABSHOP [19] stored data for later





(a)



(b)

Fig. 3. (a) Dimensions of UAV wing; (b) the mesh used in MSC PATRAN.

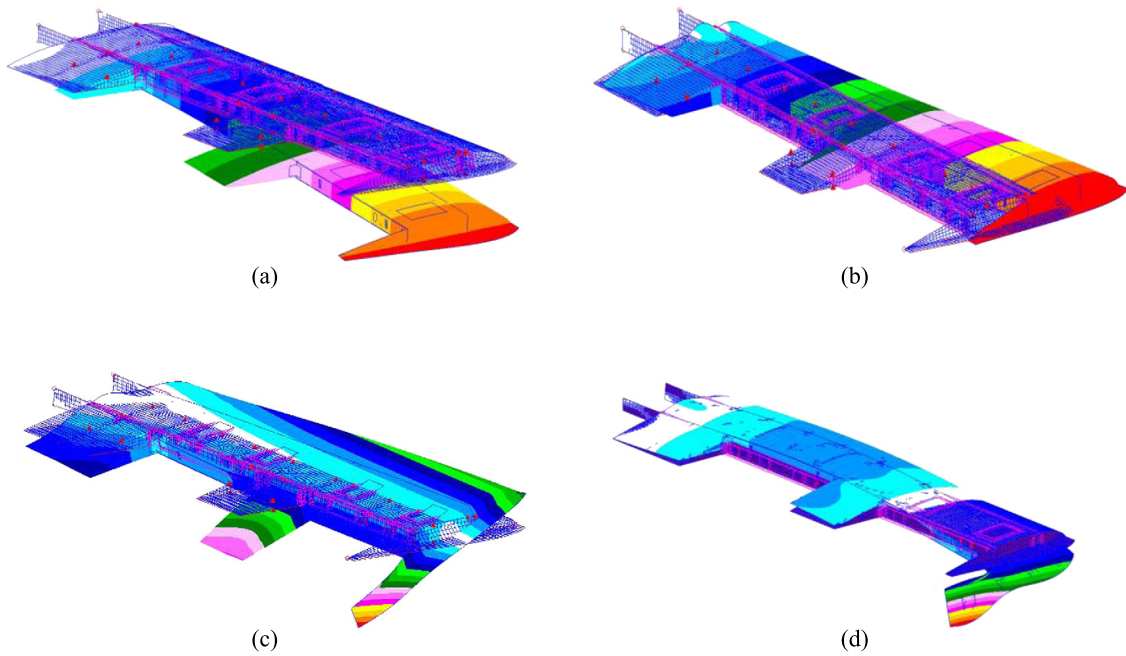


Fig. 4. Mode shapes obtained via FEA: (a) 1st out-of-plane bending [14.99 Hz], (b) 1st in-plane bending [49.87 Hz], (c) 1st torsion [62.68 Hz], (d) 2nd out-of-plane bending [94.86 Hz].

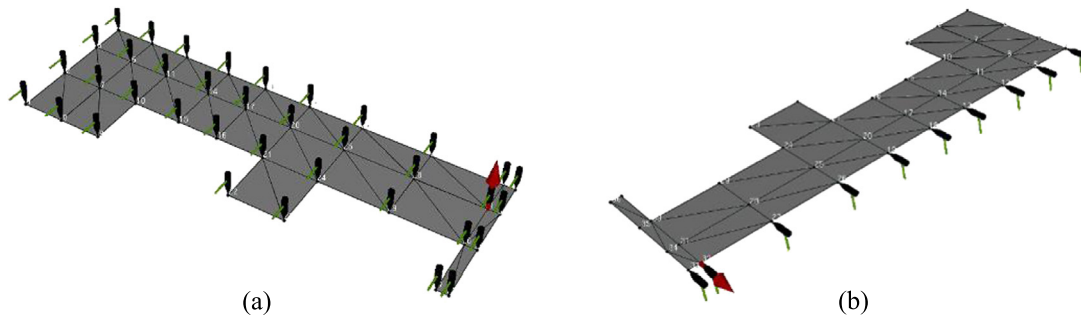


Fig. 5. Measurement locations: (a) out-of-plane, (b) in-plane (roving Hammer test).

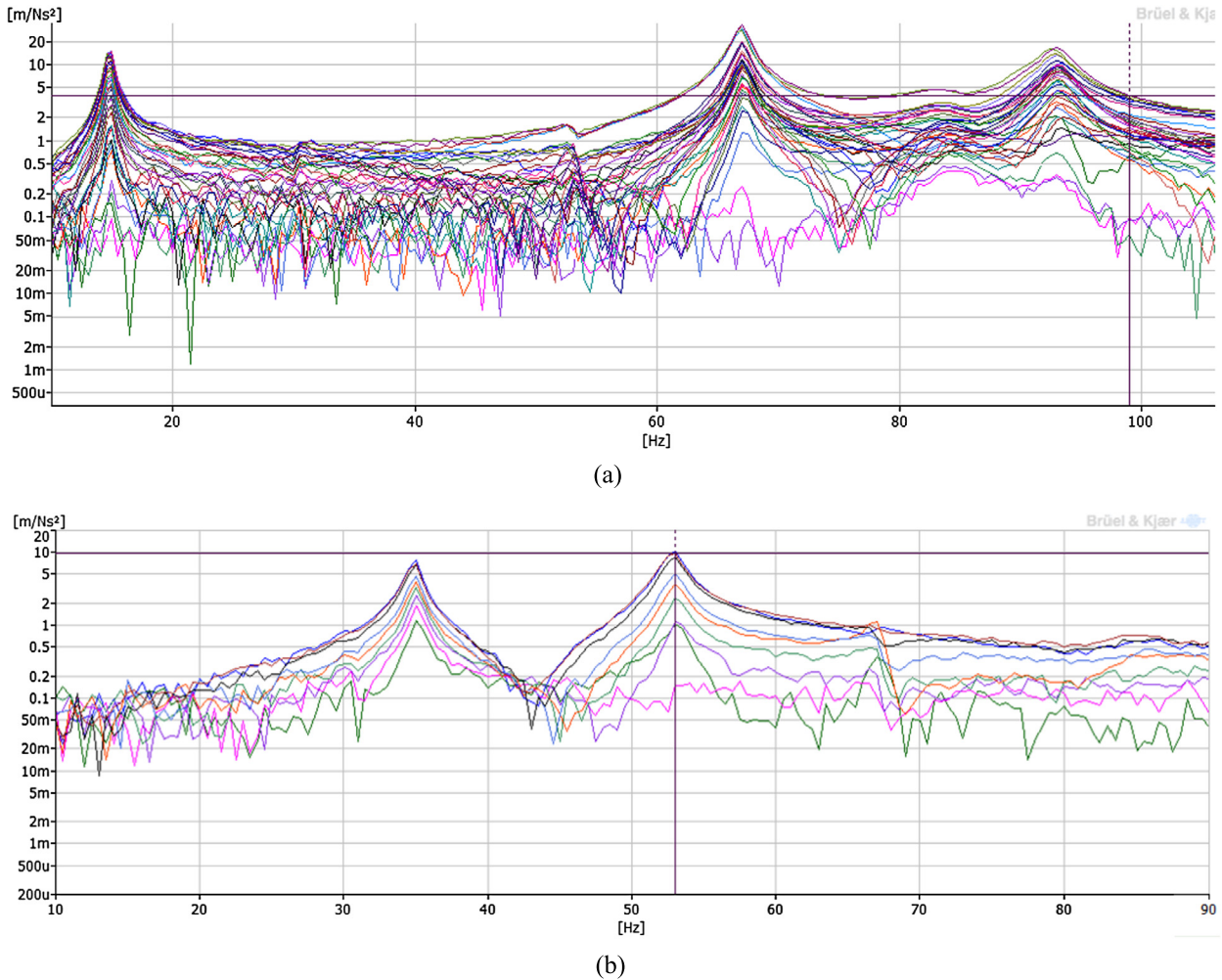


Fig. 6. Accelerance FRFs plots: (a) out-of-plane, (b) in-plane (roving Hammer test).

post processing (Modal Analysis) stage using B&K Pulse© Reflex [21] software package (Figs. 5–7).

### 3.3. Validation and model updating of the UAV wing

Finite element models (numerical model of real structures) most of the time cannot perfectly represent the actual structure. Error in material properties, neglecting changes in local material properties, uncertain boundary condition modelling, errors in model dimensions, and modelling nonlinear behaviour of structure with linear finite elements can be considered as some of those reasons. Consequences of using incorrect material proper-

ties can be decreased by applying a model updating where global material stiffness and mass values are changed. Besides, by applying a model updating which targets the local material stiffness and mass values can fix issues like disregarding local material property changes and uncertain boundary condition modelling.

Before updating the model it is advantageous to perform a correlation analysis to compare the modal characteristics of two different models i.e. FEM and the test model. FEMTools [22] software is used to update the model. As there would be no indication of the exact properties of UAV wing while modelling, standard values of aluminium were considered. So the wing's global material prop-

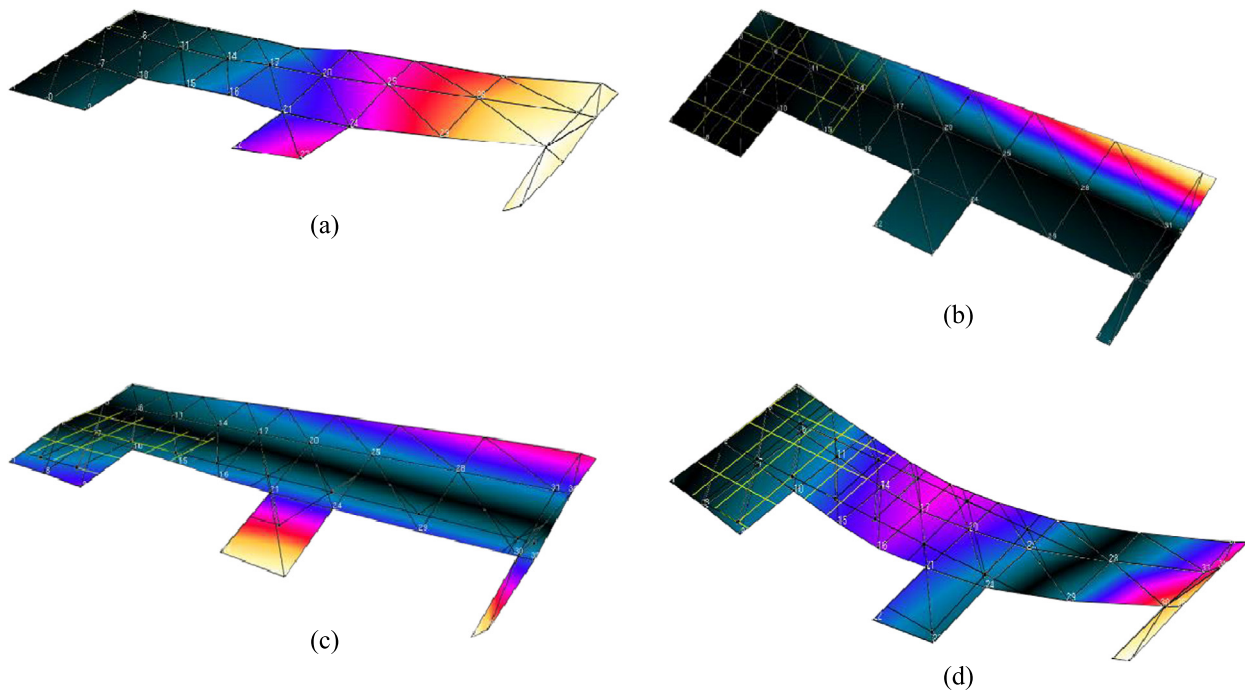


**Fig. 7.** Mode shapes obtained via EMA: (a) 1st out-of-plane bending [14.99 Hz], (b) 1st in-plane bending [49.87 Hz], (c) 1st torsion [62.68 Hz], (d) 2nd out-of-plane bending [94.86 Hz].

**Table 2**  
Model updating results.

Mode shape	FE natural frequencies – before (Hz)	FE natural frequencies – after (Hz)	EMA resonance frequencies (Hz)	% $\Delta\omega$ before	% $\Delta\omega$ after
1st Out of Plane Bending	14.99	14.88	14.85	0.93	0.20
1st In-Plane Bending	49.87	50.34	52.50	–5.27	–4.29
1st Torsion	62.67	63.12	67.29	–7.37	–6.61
2nd Out of Plane Bending	94.86	94.23	94.03	0.87	0.21

erties in model update are chosen as changing materials (where stiffness [68.9–73.1 GPa], density [2660–2851 kg/m<sup>3</sup>] are varying in these ranges) and as response parameters, natural frequencies are selected. It is observed that after several iterations, the obtained natural frequencies of FE model will get closer to those of test model. The results of the model updating are represented in Table 2.

A new set of locations for transducers in each iteration is generated during optimization phase. The new modal characteristics of the UAV wing is determined by re-meshing of existing finite element model. MATLAB script is used to perform Re-meshing process by changing existing finite element model mesh. The script will create zero dimensional point elements on candidate transducer's locations first, then assigns a lumped mass property to these locations which carry mass information of transducers. Besides it selects these locations as master degrees of freedom (ASET) to use in Guyan model reduction. Since genetic algorithm mimics nature evolutionary behaviour, it mutates and evolves in each iteration. Thus, there must be an automated process which evaluates objective and constraint functions for each solution of population. Re-meshing and re-analysis of baseline FEM will evaluate the objective function related with the error in prediction of the modal characteristics of the wing. 6 computers were selected as workers in a distributed computing cluster and it was setup using parallel computing toolbox of MATLAB. Using the cluster, a fourfold increase in computation power can be observed.

Optimization was performed using global optimization toolbox of MATLAB. Taking into account the limits of design variables, they (design variables corresponding to each member) were sent to objective and constraint functions. There are calls to external finite element solver (MSC© NASTRAN) in these objective and constraint functions. Regular expression library in MATLAB is used to feed back the Result from solver into these functions and at the end objective values and constraint violations of each member will be returned to genetic algorithm main code by these functions.

#### 4. Multi-objective optimization using genetic algorithm

Darwinian evolution can be represented mathematically in forms of a heuristic evolutionary optimization algorithm which is called genetic algorithm (GA). In Darwinian evolution it is assumed that a population composed of individuals will fight with each other and the individuals with highest fitness will survive and let to mate with other fit individuals. At the end of this process the less fit will vanish and the fit individuals will mate and produce offspring's which inherit part of their DNA strands. Genetic algorithm a mathematical representation of this natural behaviour is extensively used for optimization processes in mathematics and engineering science disciplines. In this method first a random initial population is created which is composed of several individuals which are called chromosomes. Each indi-

vidual contains all design variables of optimization problem in one of encoding formats (the most popular one is binary encoding). Each individual is evaluated by using constraint function (if there exist any) and objective function. A fitness value is assigned to each individual which then is used in selection of individuals of the next generation. During selection usually half of the population is eliminated. The eliminated half is replaced then with new offspring's created by the fit half of the population. This process will continue generation and generation until one of stopping criteria are reached. In optimization problems like this which has more than one conflicting objective function, a multi-objective approach is usually applied. In multi-objective optimization, an optimal solution is obtained with trade-offs between two or more objective functions. In objective functions domain space, non-dominated solutions (solutions in which one objective can't get improved without degrading other objectives) are placed over Pareto frontier line. These non-dominated solutions are presented as final optimal solutions to decision maker for final selection as a trade-off study. For example in design of an aerial vehicle at least performance and fuel consumption are selected as two conflicting objective functions and they are optimized using multi-objective optimization. Since optimization problem in this study has four conflicting objectives, multi-objective optimization is done and final optimal solutions are left as a trade-off study to designer.

#### 4.1. Objective functions

In this study simultaneous optimization of the number, name, and position of transducers is formulated as a multi-objective optimization problem and then the objective functions (that need to be minimized) are selected as: (1) the error in the predictions of the first four natural frequencies of the UAV wing due to mass loading of sensors, (2) error in the mode shape observability, (3) the optimum driving point error and the total transducer cost for each mentioned case.

##### 4.1.1. Mass loading error

One problem to be encountered is the fact that the mass of transducer will change modal mass of a dynamic structure despite all the advances in manufacturing lightweight and accurate transducers. As a result, the modal parameters obtained during modal survey will change. Therefore, the position of the extra mass introduced by transducers into the system is of great importance. The regions closer to the nodal lines of all modes of interest are the most suitable locations when mass loading error is considered as the only objective function. It can be easily deduced that the addition of extra mass in those areas result in minimum modal mass alteration. Although an accelerometer located at around nodal region of a specific mode results in low signal to noise ratio, this particular accelerometer may provide higher signal to noise ratio at other modes of interest since multiple modes (i.e. the first four modes) of the wing structure are considered throughout the analyses.

The error encountered due to the mass loading is estimated using summation of squared difference between first four natural frequencies of structure with and without transducers.

$$\text{Mass Loading Error} = \sum_{k=1}^4 (\omega_k^{nt} - \omega_k^t)^2$$

$$\omega_k^{nt} = k\text{'th Natural Frequency w/o transducer}$$

$$\omega_k^t = k\text{'th natural frequency w/o transducer} \quad (8)$$

##### 4.1.2. Mode shape observability error

It is very important to place the accelerometers on areas on the structure which have the highest movement and also avoid the nodal lines in all modes of interest, in order to detect and/or distinguish mode shapes of interest with higher signal to noise ratio in test results. In finite element order reduction algorithms like Guyan reduction, active degrees of freedom must usually be selected from areas with highest modal constant in all modes of interest in order to have the highest possible correlation of mode shapes between reduced and full finite element model. To achieve this, full finite element model is reduced using candidate accelerometers locations as master degree of freedom by Guyan reduction scheme and a cross correlation performed between mode shapes of full finite element model and reduced one using cross MAC (Modal Assurance Criterion) matrix. Inverse of trace of cross MAC matrix is used as mode shape observability error.

$$\text{Cross MAC Matrix} = \frac{|\varnothing_R^T \varnothing_F|^2}{|\varnothing_R^T \varnothing_R| |\varnothing_F^T \varnothing_F|}$$

$$\varnothing_F = \text{Mass Normalized Modal Matrix of Full FEM}$$

$$\varnothing_R = \text{Mass Normalized Modal Matrix of Reduced FEM}$$

$$\text{Mode Shape Observability Error} = \frac{1}{\text{trace}(\text{CrossMACMatrix})} \quad (9)$$

##### 4.1.3. Optimum driving point error

While exciting structure via impact hammer or modal shaker, there are several aspects which needs to take care of. When modal shake is attached to structure, its stinger will hinder motion of structure at that point by introducing extra stiffness. Also since force transducer has a mass, it will introduce new inertial forces into systems. It is beneficial to excite structure from places with minimum acceleration in all modes of interest. When impact hammer is used, location with higher velocity must avoided since the probability of double impact is high. So for excitation locations, areas with minimum acceleration and velocity in all modes of interest is preferred. To find those locations, minimum value of ADDOFV and ADDOFA are used (Equation (6)) for error of impact hammer and modal shaker respectively.

#### 4.2. Constraint functions

Seven constraints which are used in all of optimizations are listed below.

$AVAIL_i$  = its elements shows whether

that specific transducers is selected or not and whether it's in in-plane or out-of-plane direction (0: not selected, 1: in-plane, 2: out-of-plane)  $i = 1, \dots, 15$  (number of available transducers)

$ACC_i$  = its elements shows whether

that specific transducers is accelerometer or not  $i = 1, \dots, 15$  (number of available transducers)

$FT_i$  = its elements shows whether








that specific transducers is force transducer or not  $i = 1, \dots, 15$  (number of available transducers)

$CH_i$  = its elements shows number

of occupied channels in data acquisition device by that transducer  $i = 1, \dots, 15$  (number of available transducers)



**Table 3**  
Available equipment for EMA.

Transducer type model (number)	Price (\$)	Image	# of occupied channels	Mass (gr)
Single axis accelerometer B&K 4517-002 (5)	762		1	0.7
Single axis accelerometer B&K 4508-B (5)	630		1	4.8
Triple axis accelerometer B&K 4524 (1)	2197		3	4.8
Triple axis accelerometer B&K 4506-B (1)	1190		3	15.0
Modal Shaker's force transducer B&K 8230-002 (1)	1132		1	30.2
Impedance head B&K 8001 (1)	3165		2	29.0
Impact Hammer's force transducer B&K 8206 (1)	1684		1	0.0 (Contactless)

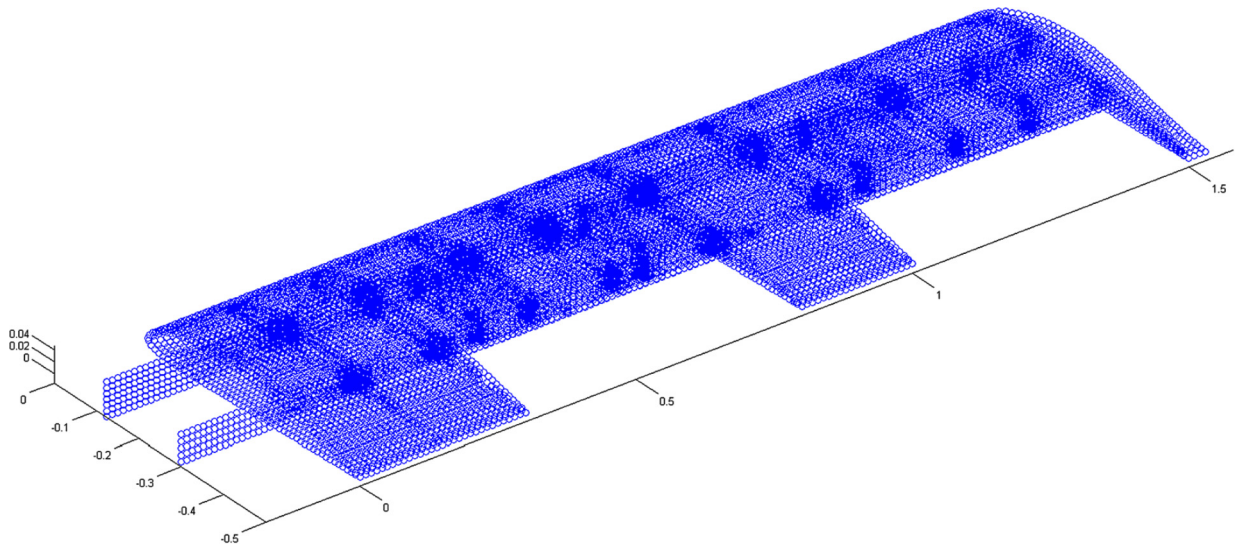


**Fig. 8.** Candidate transducers locations (all grid points).

In case of impedance head, FT and ACC are both one.

- i. Transducers must not be located on areas near the clamped part of the wing which has no skin.

$$v_i \geq L$$

$$v_i = 1 \dots 15 \left( \begin{array}{l} \text{spanwise distance from middle} \\ \text{of transducer to clamp side} \\ 15 = \text{number of available transducers} \end{array} \right)$$

$L$  = unskinned spars length

- ii. At least one accelerometer and one force transducer must be selected.

$$\sum_{i=1}^{15} \text{step\_function}(AVAIL_i - 1) * (ACC_i + FT_i) \geq 2$$

- iii. Minimum distance between transducers must not exceed the diameter of the largest transducer.

$$\sum_{\substack{i=1 \\ j=1}}^{\substack{i=15 \\ j=15}} \sqrt{(x_i - x_j)^2 + (y_i - y_j)^2 + (z_i - z_j)^2} \geq D_{Largest}$$

$x_{i,j}$  = x coordinate of centre of transducer

$y_{i,j}$  = y coordinate of centre of transducer

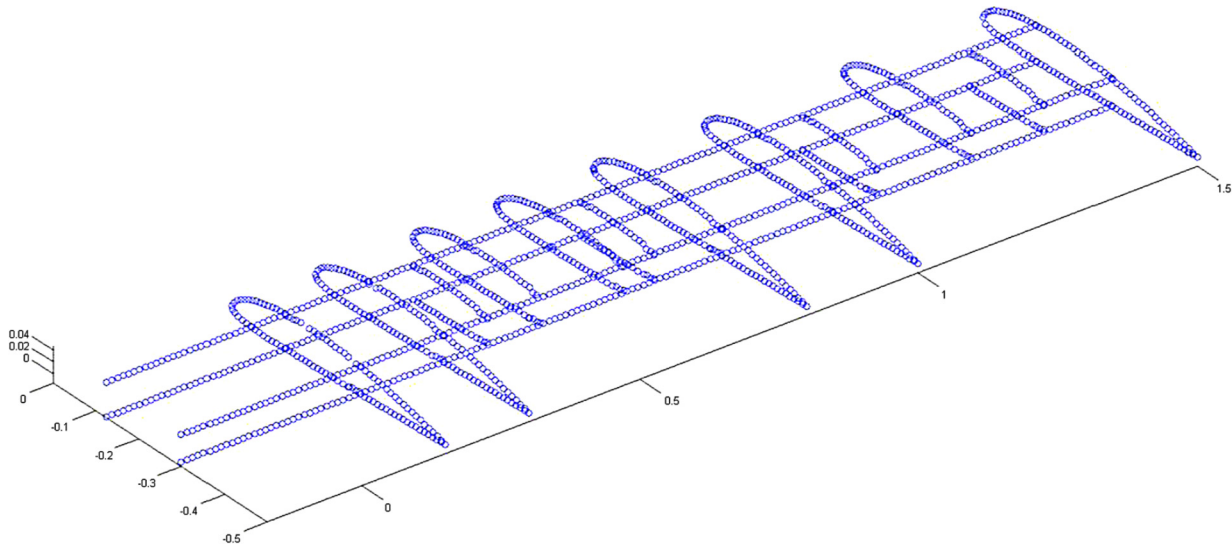


Fig. 9. Candidate transducers locations (selected grid points).

$z_{i,j}$  = z coordinate of centre of transducer

$D_{Largest}$  = largest transducer diameter

- iv. Number of occupied channels by transducers must not exceed six. (data acquisition device has maximum of six channels)

$$\sum_{i=1}^{15} \text{step\_function}(AVAIL_i - 1) * CH_i \leq 6$$

- v. Only one force transducer must be selected, because the test setup (roving hammer) is a SIMO (single-input and multiple-output) system.

$$\sum_{i=13}^{15} \text{step\_function}(AVAIL_i - 1) \leq 1$$

$i = 13, 14, 15$  are indices of force transducers

- vi. At least one accelerometer in both in-plane and out-of-plane directions to capture both in plane and out of plane mode shapes.

at least one  $AVAIL_i$  with value of one and

another  $AVAIL_i$  with value of 2

$i = 1, \dots, 15$  (number of available transducers)

- vii. In order to make modal test easier for test engineer, impact hammer location must be on areas over upper skin and modal shaker location must be on areas over lower skin of wing.

impact hammer vertical distance from wing midsurface > 0

modal shaker vertical distance from wing midsurface < 0

#### 4.3. Design variables

There are fifteen available transducers used in this study. In Table 3, transducers' type, model, number, image, price, mass and channel usage are listed. For each of these transducers two design variables are assigned. One variable is a binary variable that shows the use of that transducer and its measurement direction which is either zero, one or two. (0: not selected, 1: selected and

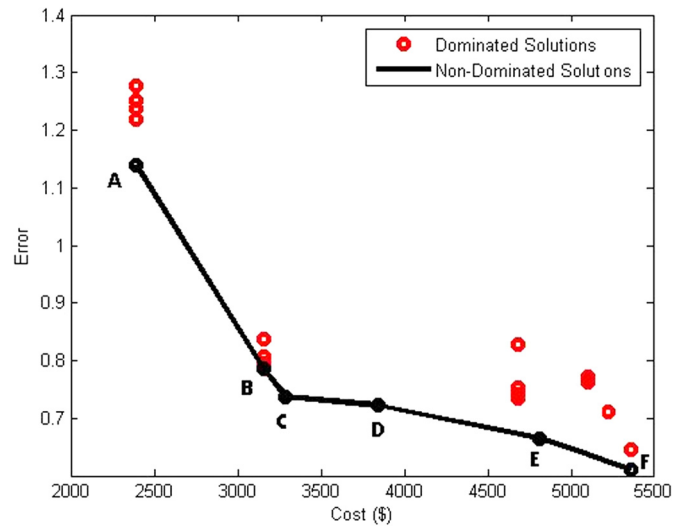


Fig. 10. Pareto frontier curve and selected non-dominant solutions (total error).

in-plane, 2: selected and out-of-plane). The other variables is a discrete variable which is node number of corresponding transducer. Therefore, there are 30 discrete design variables which are used in this optimization problem. There are 18,904 grid points (Fig. 8) in wing FE model but transducers must located on exterior grid points not interior ones. Also to avoid capturing local mode shapes (Usually on skin between spars and ribs), only exterior points which are located over ribs and spars are chosen as candidate transducer location (Fig. 9). This reduces the number of grids to 1511, which in return reduces FEA calculations runtime tremendously.

#### 5. Optimization results

Multi-objective optimization problems usually will not present only single optimum solution. In fact they offer several optimum solutions. Some of these solutions are dominated by other solutions because of higher values in all of objective functions and the rest are called non-dominated solutions. A curve which passes through all of these non-dominant solutions in objective function space is called Pareto frontier curve.

**Table 4**  
Total error and cost of Pareto frontier solutions (total error).

Configuration	ML error <sup>a</sup>	MSO error <sup>a</sup>	ODP error <sup>a</sup>	Total error	Cost (\$)
A	0.0836	1.0538	0.0020	1.1394	2392
B	0.0754	0.7086	0.0017	0.7857	3155
C	0.0405	0.6941	0.0030	0.7376	3288
D	0.0400	0.6803	0.0022	0.7225	3839
E	0.1301	0.5317	0.0028	0.6645	4813
F	0.0594	0.5382	0.0134	0.6110	5364

<sup>a</sup> ML: Mass loading MSO: Mode shape observability ODP: Optimum driving point.

Since in equivalent error calculation all of errors are summed without using any weighting, most error (MSO Error) will get minimized more than other two non-dominant errors (ODP and ML Errors). Non-dominant errors are kept at a minimum level. In configuration A because of cost constraint only two accelerometers (cheapest and heaviest) and modal shaker force transducer (cheapest) are selected. One accelerometer is pointed in out-of-plane direction and other is pointed in in-plane direction to make 1st in-plane and out-of-plane bending modes distinguishable in test results (Fig. 10 and Table 4).

In configuration B with an increased cost limit, third accelerometer (4517-002) is selected which is expensive and light. In con-

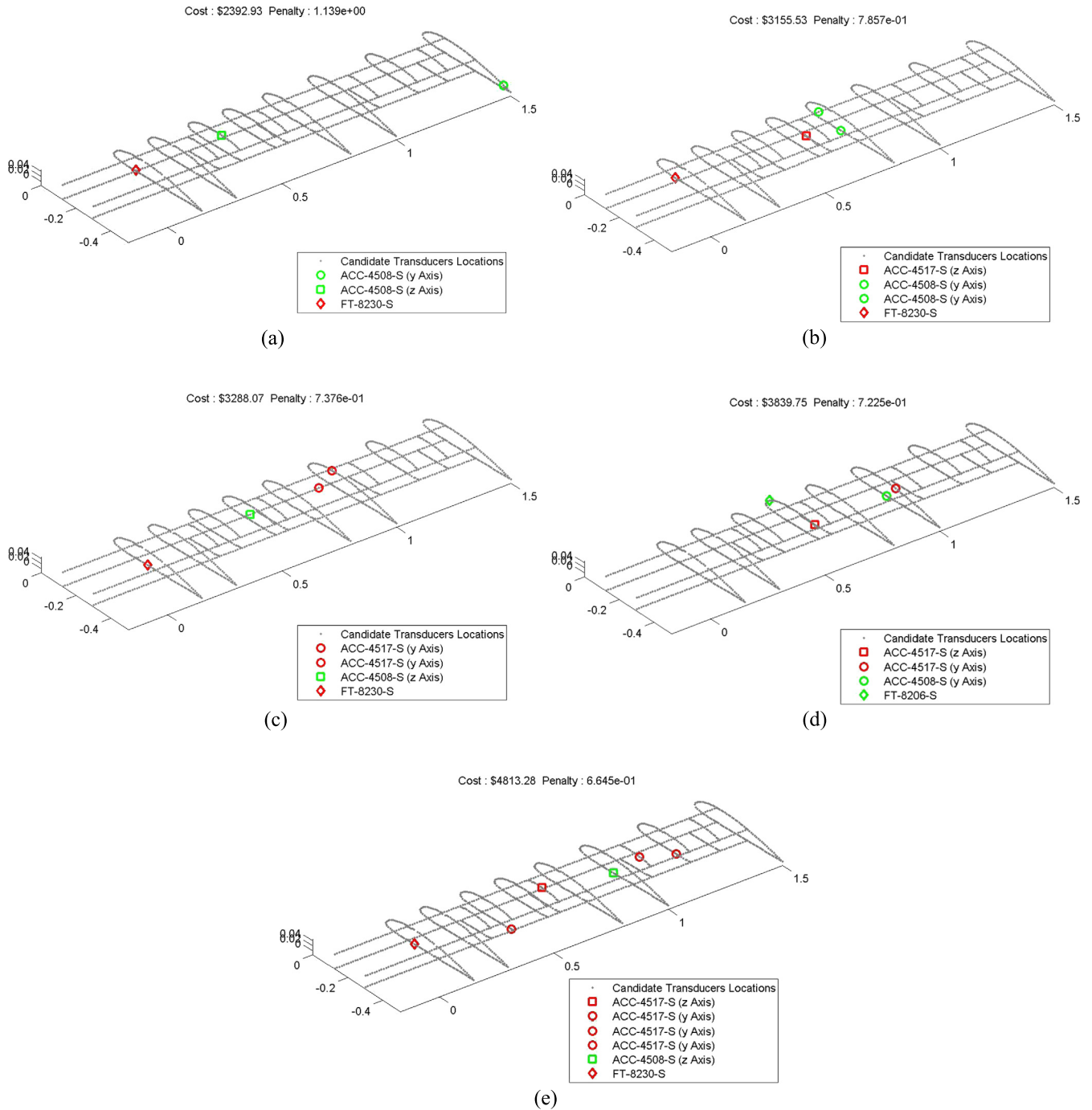
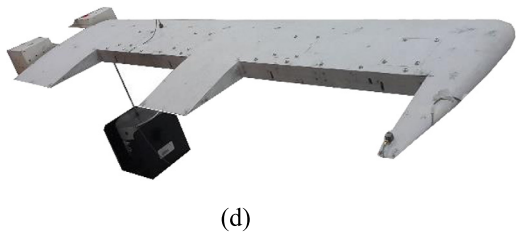
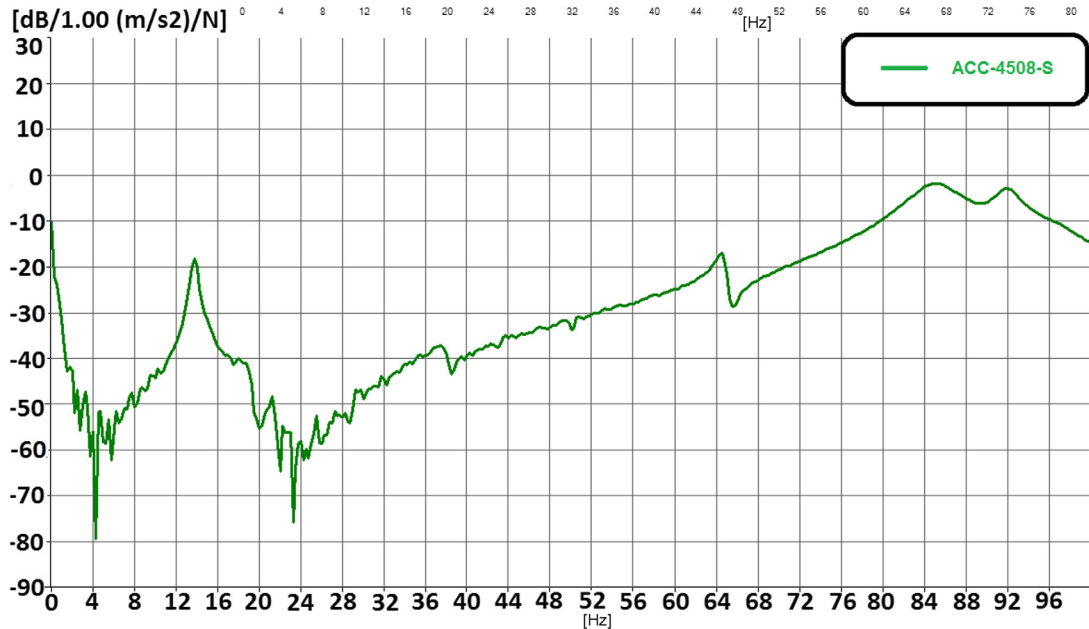
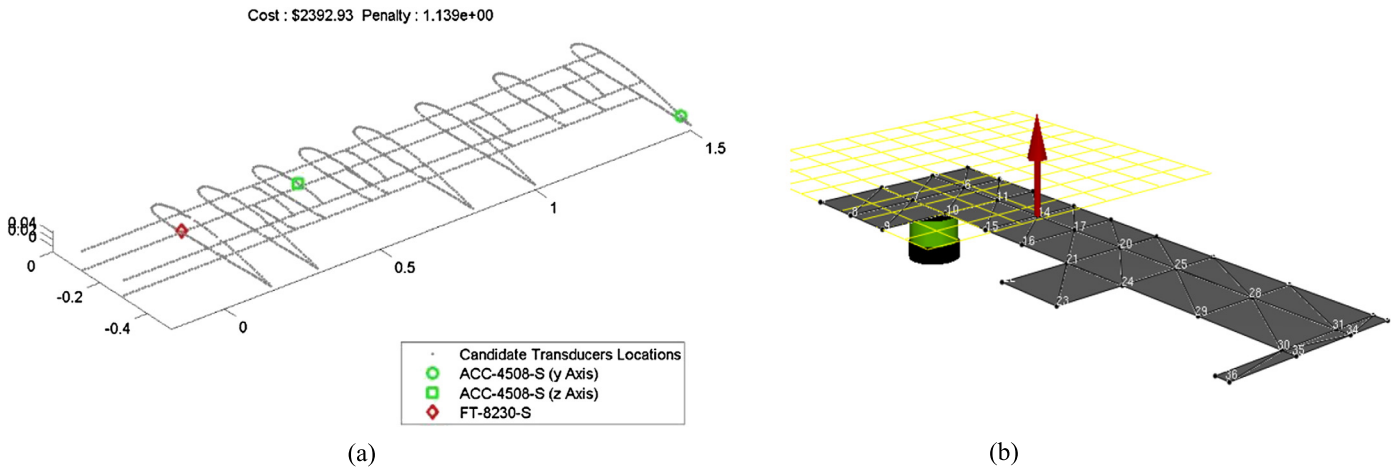


**Fig. 11.** Locations of transducers in candidate configurations from Pareto frontier (total error): (a) Configuration A; (b) configuration B; (c) configuration C; (d) configuration D; (e) configuration E; (f) configuration F.

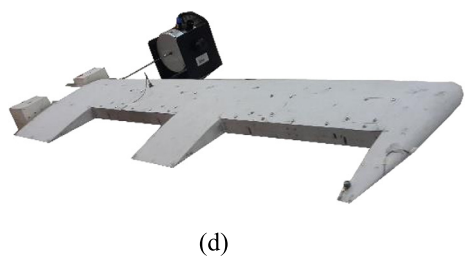
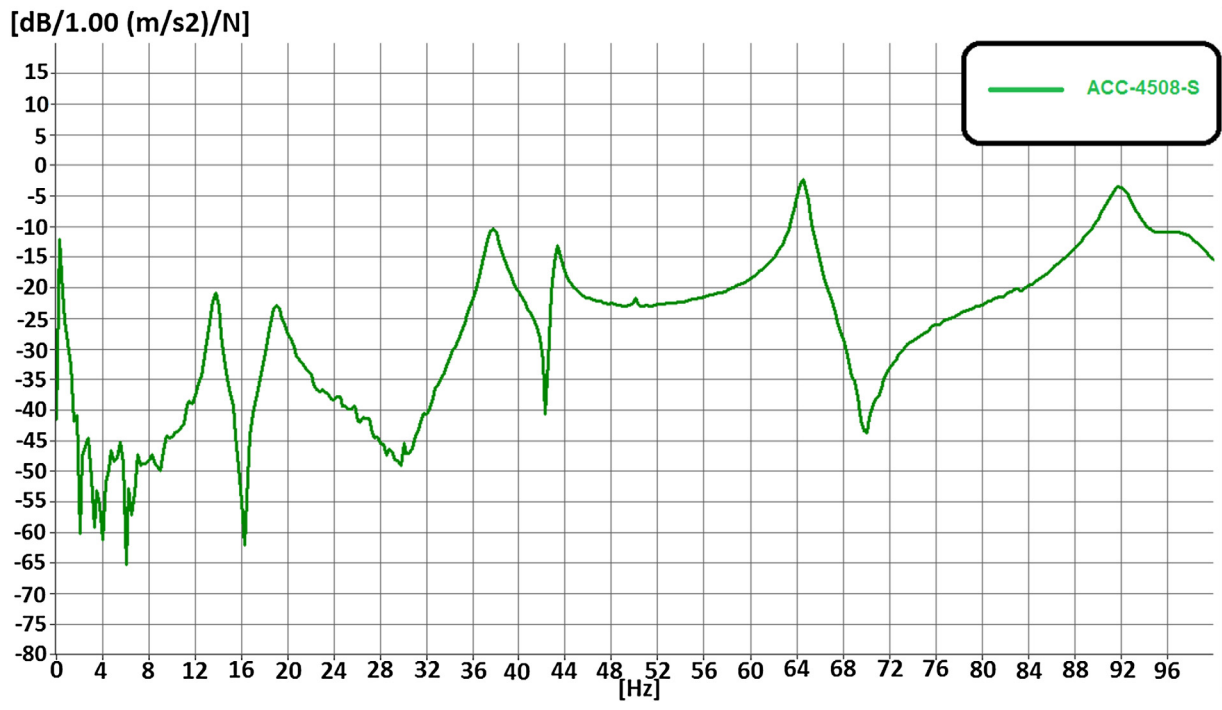
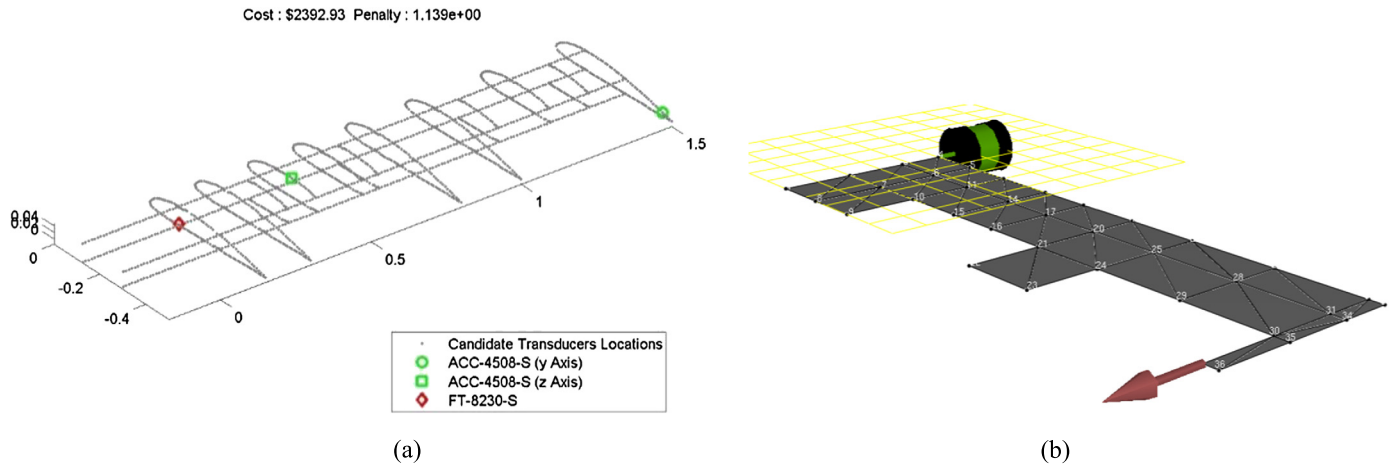


Configuration	Resonance Frequencies[Hz]		
	1. Mode	2. Mode	3. Mode
Total Error (A)	13.75	64.50	92.00

(e)

Fig. 12. Total error – configuration a [out of plane] [UAV wing]. (a) Configuration obtained from optimization; (b) Configuration in B&K modal test consultant; (c) acceleration FRF; (d) test setup (e); resonance frequencies obtained.

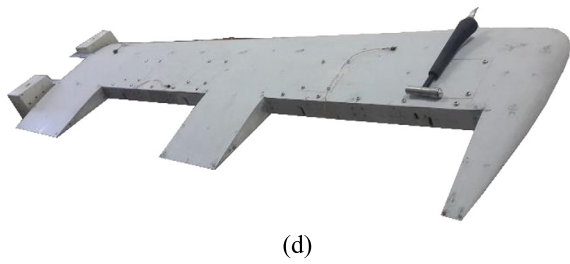
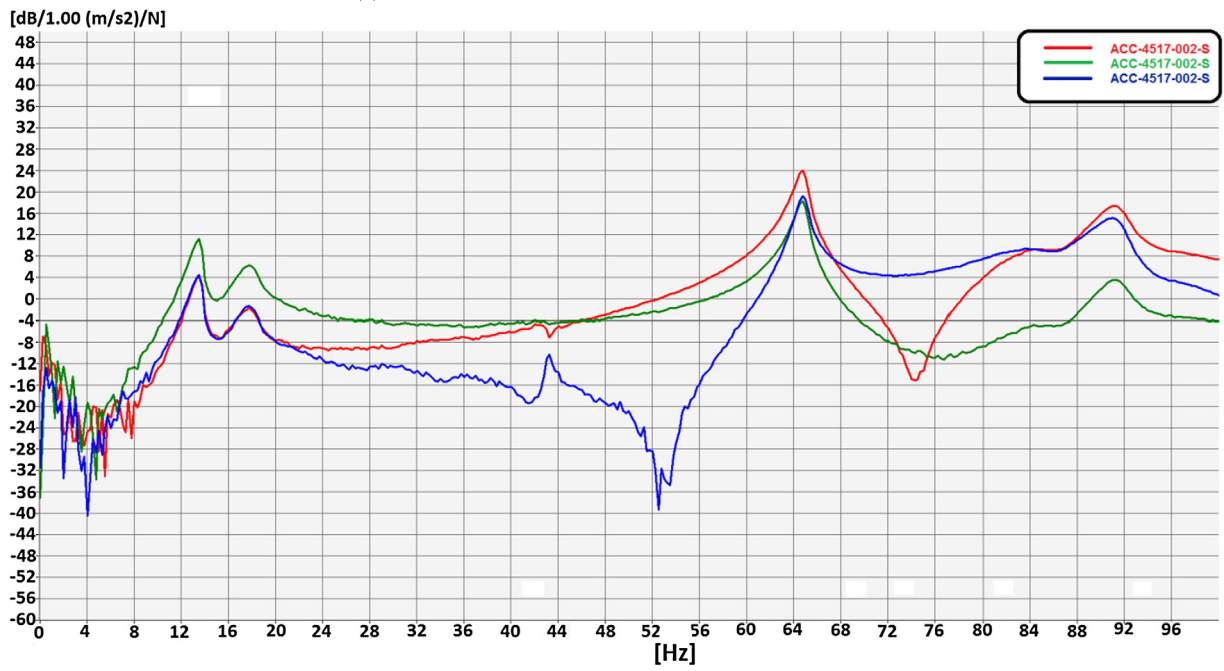
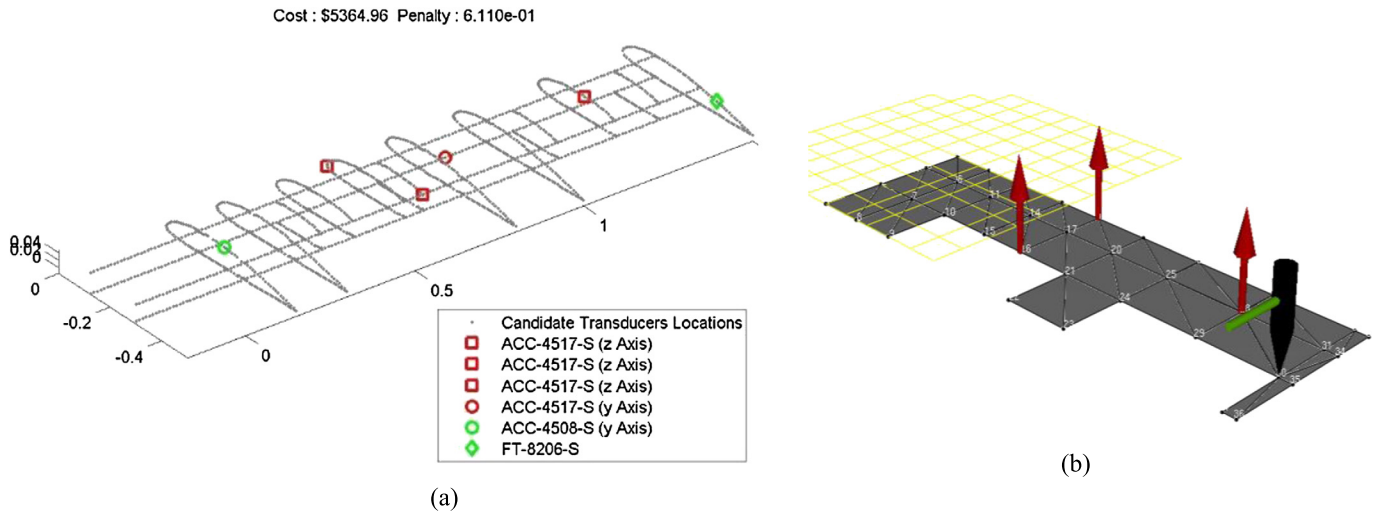




Resonance	
Configuration	Frequencies[Hz]
	1. Mode
Total Error (A)	43.25

(e)

**Fig. 13.** Total error – configuration A [in-plane] [UAV wing]. (a) Configuration obtained from optimization; (b) configuration in B&K modal test consultant; (c) acceleration FRF; (d) test setup; (e) resonance frequencies obtained.



Resonance			
Configuration	Frequencies[Hz]		
	1.	2.	3.
	Mode	Mode	Mode
Total Error (F)	13.50	64.75	91.25

(e)

Fig. 14. Total error – configuration F [out of plane] [UAV wing]. (a) Configuration obtained from optimization; (b) configuration in B&K modal test consultant; (c) acceleration FRF; (d) test setup; (e) resonance frequencies obtained; (f) mode shapes observed from one measurement. (For interpretation of the colours in this figure, the reader is referred to the web version of this article.)

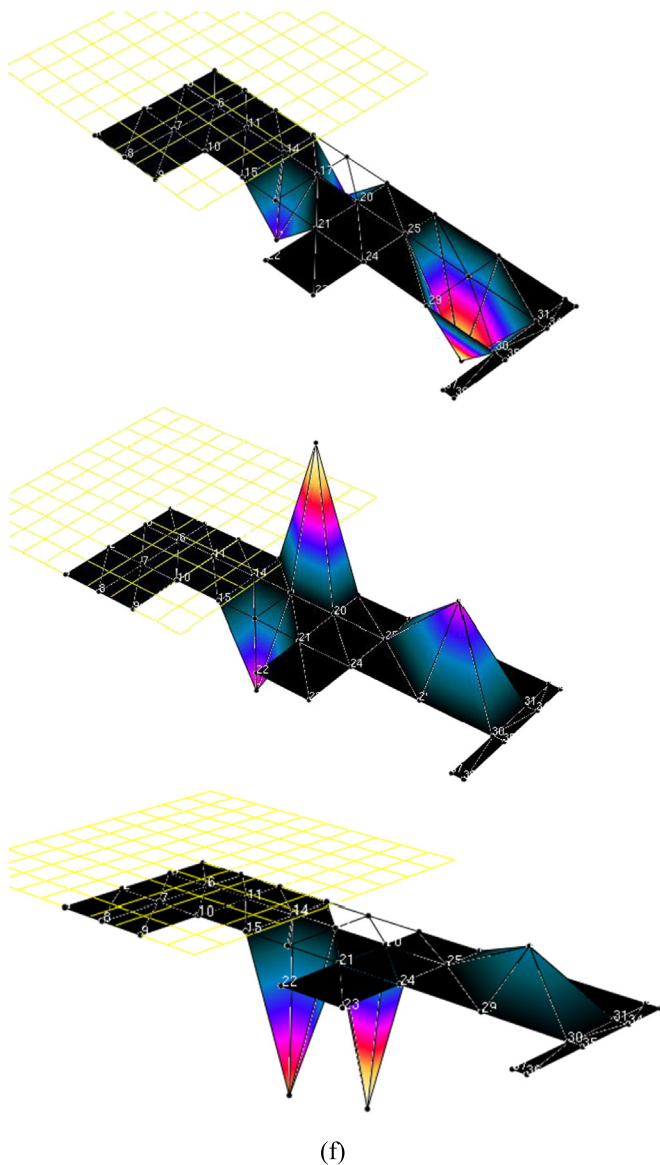


Fig. 14. (continued)

figuration C, instead of one accelerometer, two of them are chosen as miniature one (4517-002). With another further price increase force transducer is changed from modal shaker to impact hammer which is more expensive. In configuration F three miniature accelerometers (4517-002) are located in a triangular shape to capture 1st and 2nd out of plane bending and 1st torsion mode shapes. Two accelerometers are directed in in-plane direction to capture 1st in-plane bending mode shape. Impact hammer force transducer is also chosen because it is the most expensive one. Since these results may be local minimum, further optimization may find better local minimums or even global minimum (Fig. 11).

## 6. Verification of optimization results via modal test

This part verifies cheapest and most expensive configurations over Pareto frontier curve using experimental modal analysis. In verification part, negligible effect of mass loading and observability of mode shape are checked. In figures (Figs. 12–15), upper left corner shows location of transducers over wing, upper right corner shows configuration used in modal test consultant of LABSHOP

software, middle shows acceleration frequency response function, lower left corner shows wing with test equipment and lower right corner shows natural frequencies. Since the most expensive configuration is a SIMO system, figures which shows mode shape observability are also shown. But this is not shown in cheapest configuration because it is a SISO system and mode shape observability will not give any valuable information about mode shapes of structure.

## 7. Conclusion

A good pre-test analysis will reduce time and cost of an experimental modal test and increase quality of test results. A multi-objective optimization was performed to find optimum number, type and locations of transducers used in modal test of an UAV wing. There are three important problems which test engineer encounter during modal test are, mass loading error, mode shape observability error and optimum driving point error. Mass loading error is a consequence of addition of external masses to original structure over areas with high acceleration. This error can be minimized by placing accelerometers near or over nodal lines or close to fixture side of wing. Mode shape observability error shows how much mode shapes are distinguishable from modal test results.

Optimum driving point is used to find locations on structure with minimum velocity and acceleration. Hitting structure with impact hammer over areas with high velocity leads to double-hit problem and exciting structure from areas with high acceleration leads to shaker-structure interaction problem (local stiffening). In optimization MSC© NASTRAN finite element solver and multi-objective optimization toolbox of MATLAB were used. At the end of optimization a Pareto frontier was plotted. These plots are very helpful to a test engineer. All of solutions over Pareto frontier curve were arranged in a way to capture all mode shapes of interest with minimum possible mass loading error. It is evident from results that four accelerometers would suffice for this purpose. ODP error caused the excitation location to be near clamped side of wing with minimum velocity and acceleration. In verification stage configuration A and F shows a high amplitude response over frequencies near resonance and that's a sign of high signal to noise ratio. It is also evident from verification of configuration F that all mode shapes of interest are observable with only one SIMO test. Finally, it is observed from the optimization and the experimental verification results that the proposed approach is a realizable one which could be used in the ground vibration tests of aircraft structures.

## Conflict of interest statement

There is no conflict of interest.

## Acknowledgements

The authors gratefully acknowledge the funding provided by The Scientific and Technological Research Council of Turkey (TUBITAK) with project 112M845.

## References

- [1] P.C. Shah, F.E. Udawadia, A methodology for optimal sensor locations for identification of dynamic systems, *J. Appl. Mech.* 45 (1978) 188.
- [2] D.C. Kanner, Sensor placement for on-orbit modal identification and correlation of large space structures, in: 1990 Am. Control Conf., vol. 14, 1990, pp. 251–259.
- [3] L. Yao, W.a. Sethares, D.C. Kammer, Sensor placement for on-orbit modal identification of large space structure via a genetic algorithm, in: Proceedings 1992 IEEE Int. Conf. Syst. Eng., vol. 31, 1992, pp. 1922–1928.
- [4] F.E. Udawadia, Methodology for optimum sensor locations for parameter identification in dynamic systems, *J. Eng. Mech.* 120 (2) (1994) 368–390.

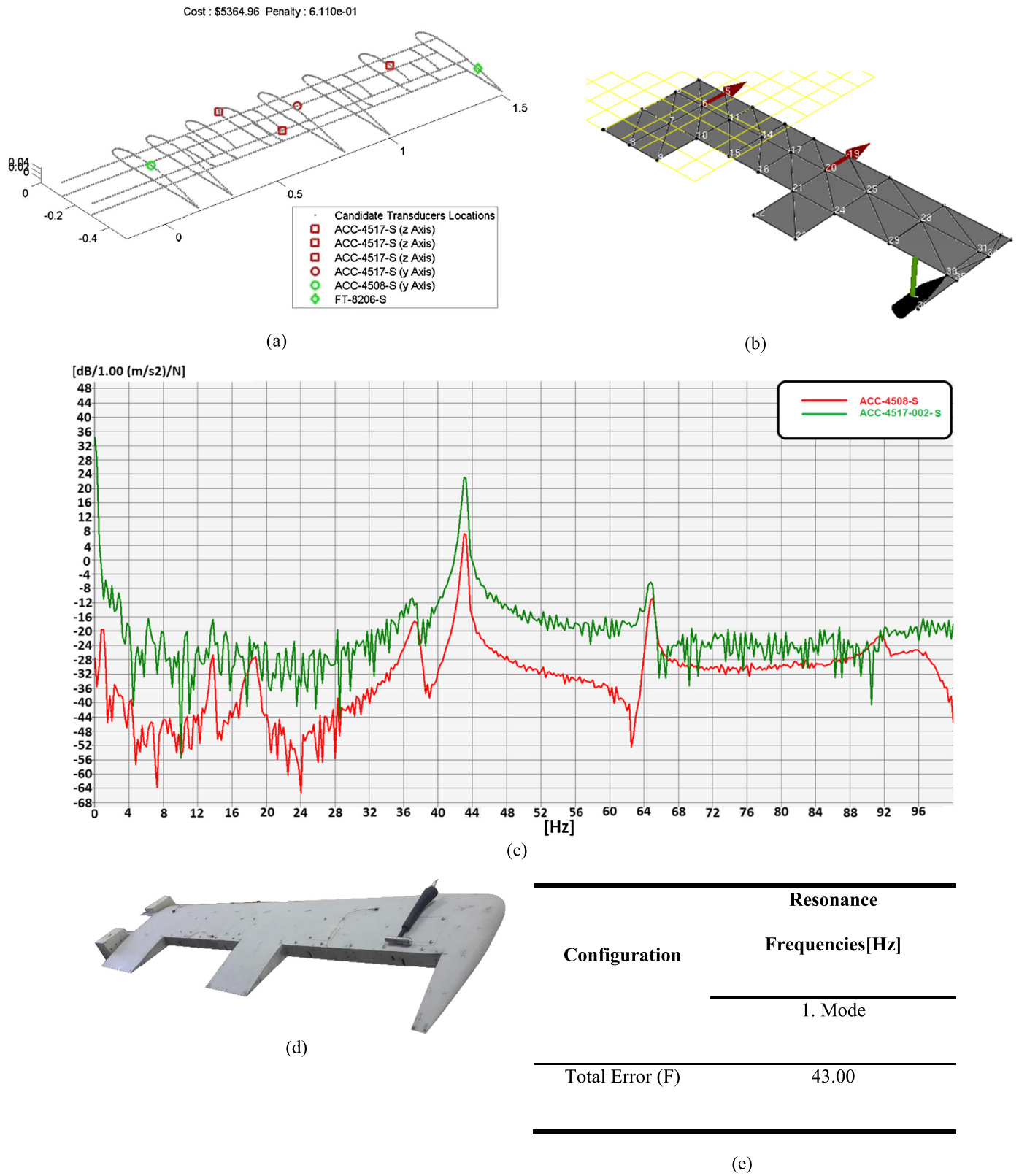


Fig. 15. Total error – configuration F [in-plane] [UAV wing]. (a) Configuration obtained from optimization; (b) configuration in B&K modal test consultant; (c) acceleration FRF; (d) test setup; (e) resonance frequencies obtained. (For interpretation of the colours in this figure, the reader is referred to the web version of this article.)



- [5] P.H. Kirkegaard, R. Brincker, On the optimal location of sensors for parametric identification of linear structural systems, *Mech. Syst. Signal Process.* 8 (1994) 639–647.
- [6] J.E.T. Penny, M.I. Friswell, S.D. Garvey, Automatic choice of measurement locations for dynamic testing, *AIAA J.* 32 (1994) 407–414.
- [7] R.M. Rao, G. Anandakumar, Optimal placement of sensors for structural system identification and health monitoring using a hybrid swarm intelligence technique, *Smart Mater. Struct.* 16 (6) (2007) 2658–2672.
- [8] T. Van Langenhove, M. Brughmans, Using MSC/Nastran and LMS/Pretest to find an optimal sensor placement for modal identification and correlation of aerospace structures, in: *LMS International Belgium*, 1999.
- [9] I.T.J. Peck, A DMAP program for the selection of accelerometer locations in MSC/NASTRAN, in: *Proceedings of the 45th AIAA/ASME/ASCE/AHS/ASC Structures*, 2004.
- [10] MATLAB, online available: <http://www.mathworks.com/products/matlab/?refresh=true>.
- [11] MSC® NASTRAN, online available: <http://www.mscsoftware.com/product/msc-nastran>.
- [12] N. Pedramasl, M. Sahin, E. Acar, Simulation-based optimal sensor/actuator positioning on a fin-like structure, in: *16th AIAA/ISSMO Multidisciplinary Analysis and Optimization Conference*, Dallas, TX, ABD, 22–26 Haziran 2015, Paper No: AIAA 2015-2489.
- [13] N. Imamovic, *Validation of Large Structural Dynamics Models Using Modal Test Data*, 1998.
- [14] Z.-Q. Qu, *Model Order Reduction Techniques with Applications in Finite Element Analysis*, 2004, pp. 47–50.
- [15] Z.-Q. Qu, *Model Order Reduction Techniques with Applications in Finite Element Analysis*, 2004, pp. 151–162.
- [16] MSC® PATRAN, online available: <http://www.mscsoftware.com/product/patran>.
- [17] 8206 – impact hammer, online available: <http://www.bksv.com/Products/transducers/vibration>.
- [18] 4517 – miniature tear-drop CCLD accelerometer, online available: <http://www.bksv.com/>.
- [19] B&K pulse labshop, online available: <http://www.bksv.com/products/pulse-analyzer/pulse-platform/pulse-labshop.aspx>.
- [20] 7753 – modal test consultant, online available: <http://www.bksv.com/products/analysis-software/vibration/structural-dynamics/classical-modal-analysis/modal-test-consultant-7753>.
- [21] B&K pulse reflex, online available: <http://www.bksv.com/Products/pulse-analyzer/pulse-platform/pulse-reflex-core.aspx>.
- [22] FEMTools, online available: <http://www.femtools.com/>.